Salivary proteins of a gall-inducing aphid and their impact on early gene responses of susceptible and resistant host-plant genotypes

Luis Portillo Lemus [1, 2] *, Jessy Tricard [1, 2] *, Jérôme Duclercq [2], Quentin Coulette [2], David Giron [3], Christophe Hano [1], Elisabeth Huguet [3], Frédéric Lamblin [1], Anas Cherqui [2] °, Aurélien Sallé [1] °

[1] Laboratoire de Biologie des Ligneux et des Grandes Cultures, INRA, Université d'Orléans, 45067, Orléans, France

[2] Ecologie et Dynamique des Systèmes Anthropisés, EDYSAN UMR CNRS-UPJV 7058, Université de Picardie Jules Verne, Amiens, France

[3] Institut de Recherche sur la Biologie de l'Insecte, UMR 7261, CNRS/Université François-Rabelais de Tours, Tours, France

* L. Portillo Lemus and J. Tricard should be considered joint first author

° A. Cherqui and A. Sallé should be considered joint senior author

Abstract

Plant manipulation by herbivores requires fine-tuned reprogramming of host metabolism, mediated by effector molecules delivered by the parasite into its host. While plant galls may represent the epitome of plant manipulation, secretomes of gall-inducers and their impact on host-plants have been rarely studied. We characterized, with transcriptomic and enzymatic approaches, salivary glands and saliva of a gall-inducing aphid, *Phloeomyzus passerinii*. Early responses to aphid saliva of plant genes belonging to different metabolic and signaling pathways were assessed *in vivo*, with poplar protoplasts, and *in planta*, in a heterologous *Arabidopsis* system. Several effectors potentially interfering with plant signaling have been identified, including binding proteins, oxidoreductases, and phosphatidylinositol phosphate kinases. Compatible interactions between protoplasts of a susceptible poplar genotype and the saliva of *P. passerinii* led to an overall downregulation of defense-related genes while an upregulation was observed during both incompatible interactions, with a resistant poplar genotype, and non-host interactions, with the saliva of *Myzus persicae*, an aphid which does not feed on poplars. Compatible interactions affected both auxin transport and homeostasis potentially leading to an intracellular accumulation of auxin, which was further supported by *in planta* assays. Our results support the hypothesis that effectors interfere with downstream signaling and phytohormone pathways.

Keywords

Effector, *Myzus persicae*, *Phloeomyzus passerinii*, plant-insect interaction, *Populus*, resistance, RT-qPCR

1. Introduction

Nutritional imbalance and defense mechanisms are major hurdles hampering plant resources exploitation by animals (Schoonhoven, Van Loon, & Dicke, 2005). To cope with this, some herbivores have evolved strategies consisting in remodeling plant tissues to turn them into optimal substrates for their development and fitness (Lieutier et al., 2017). The epitome of such plant manipulation is certainly gall induction, triggering sometimes spectacular and complex tissue reorganization resulting in new plant organs, within which parasites feed and grow (Stone & Schönrogge, 2003; Shorthouse, Wool & Raman, 2005; Giron, Huguet, Stone & Body, 2016). To adapt plant tissues to nutritional requirements of parasites and to circumvent plant defenses, gall development implies fine-tuned metabolism reprogramming, and direct modulations of both primary and secondary metabolisms of host plants have been reported for gall-inducing organisms (Giron et al., 2016). More specifically, since they are important regulators of plant growth, differentiation and defense, phytohormones are classical targets of plant-manipulating organisms, and considered key factors intimately involved in the success or failure of gall differentiation (Tooker & Helms, 2014; Giron et al., 2016).

Host metabolism hijacking by plant-manipulating organisms is considered to be mediated by effector molecules delivered into the host-plant (Hogenhout & Bos, 2011; Giron et al., 2016). Effector proteins secreted by herbivores in general have various functions, including suppression of plant defense, alteration of plant development, and manipulation of plant resources (Hogenhout & Bos, 2011; Giron et al., 2016). For gall-inducing organisms, similar functions are expected, especially disruption or diversion of hormone-dependent pathways (Tooker & Helms, 2014) and inactivation of second messengers involved in stress signaling like Ca^{2+}, reactive oxygen species (ROS) and extracellular ATP for instance (Will, Tjallingii, Thönnessen & van Bel, 2007; Guiguet et al., 2016). While there is a growing literature dealing with the identification of these effectors in herbivores, like aphids (e.g. Harmel et al., 2008; Nicholson, Hartson & Puterka, 2012; Vandermoten et al., 2014; Boulain et al., 2018), few investigations

have been performed on secretions of gall-inducing organisms, with notable exceptions of the Hessian fly (*Mayetiola destructor*, Say) and root-knot nematodes (*Meloidogyne* spp.) for instance (e.g. Zhao et al., 2015; Favery, Quentin, Jaubert-Possamai & Abad, 2016). So far, the Hessian fly is the only gall-inducing insect with a sequenced genome, and whose salivary gland transcriptome and proteome have been studied (Stuart, Chen, Shukle & Harris, 2012; Zhao et al., 2015). Candidate genes with effector functions have been detected and gene-for-gene interaction between insect strains and host-plant genotypes has been demonstrated (Stuart et al., 2012; Zhao et al., 2015; 2016). How these effectors contribute to gall induction is still unclear, but it is hypothesized that they interfere with downstream signaling and phytohormone pathways (Zhao et al., 2016).

To validate the relevance of candidate effectors for plant-insect interactions, several approaches have been used. *In planta* modulation of candidate effectors expression allowed to highlight impacts of effector proteins on physiological traits and behavior of insects and plant responses (e.g. Mutti et al., 2008; Atamian et al., 2013; Zhao et al., 2016). Alternatively, direct applications of oral secretions and saliva infiltration into host plants also gave conclusive results (e.g. De Vos & Jander, 2009; Chaudhary, Atamian, Shen, Briggs & Kaloshian, 2014). Nonetheless, probably because of their complex life cycles and generally concealed endophytic development, very few functional validation experiments have been performed with gall-inducing insects (e.g. Zhao et al., 2016). In-depth functional molecular approaches would allow to unravel the mechanisms that contribute to plant manipulation by these organisms and could possibly lead to identification of convergent mechanisms among them (Giron et al., 2016).

Here, we report the characterization of salivary proteins of *Phloeomyzus passerinii* Sign., a gall-inducing aphid colonizing poplars (Sallé, Pointeau, Bankhead-Dronnet, Bastien & Lieutier, 2017). As this insect can be easily handled under laboratory conditions, and its saliva can be collected on artificial medium, we performed innovative functional validation assays to address the impact of the saliva of a gall-inducing organism on gene responses of its host-plant. Our objectives were (i) to characterize with transcriptomic

and enzymatic approaches the salivary glands and saliva, respectively, of *P. passerinii*, (ii) to assess *in vivo*, with a RT-qPCR approach, early responses of poplar genes belonging to different metabolic and signaling pathways using protoplasts exposed to aphid saliva, and (iii) to investigate the impact of salivary extracts on specific gene expression *in planta*, in a heterologous *Arabidopsis* system. For all these steps comparative approaches have been used. The determined salivary proteins of *P. passerinii* were compared with those of a sap-feeding aphid *Myzus persicae* (Sulzer) (Harmel et al., 2008; De Vos & Jander, 2009) in order to identify proteins common to both aphid species as well as proteins specific to *P. passerinii*. To get insight into how *P. passerinii* manipulates host metabolism and stress responses to perform gall-induction, the impact of salivary extracts on gene expression has been assessed with poplar genotypes either susceptible or resistant to *P. passerinii*, i.e. during compatible and incompatible interactions, respectively. These poplar genotypes have also been exposed to salivary extracts of *M. persicae*, which led to non-host interactions since *M. persicae* does not feed on poplar.

2. Materials and Methods

2.1. Plant and insect material

Phloeomyzus passerinii is a specialist of poplars, inducing open galls in the cortical parenchyma of its host-trees and feeding on cell contents (Pointeau et al., 2012; Dardeau et al., 2014; Sallé et al., 2017). During gall induction in susceptible hosts, cell multiplication in cortical parenchyma is visible one week after the onset of aphid probing, and three weeks later thin-walled hypertrophied cells differentiate while vacuolar phenolic compounds disappear from the galled tissues (Dardeau et al., 2014). In resistant host genotypes, lignin, tannins and flavanols accumulate at the probing site one week after the onset of probing and no gall differentiation occurs subsequently. As a consequence, *P. passerinii* cannot develop on these genotypes (Dardeau et al., 2014). All individuals of *P. passerinii* used either for transcriptomic analyses of salivary glands or saliva collection originated from the same monoclonal colony established

from an apterous parthenogenetic female, collected in 2013 in Brézé (France). The colony was maintained in the laboratory on potted stem cuttings of I-214, a *Populus x canadensis* Moench. genotype, under 20 ± 1 °C, 70 ± 10% relative humidity and 16/8 h light/dark cycles. The green peach aphid, *Myzus persicae* is a sap-feeder and a generalist aphid. Nonetheless, its host range does not include poplars, and preliminary establishment attempts confirmed that it cannot settle and develop on poplars (data not shown). Therefore non-host interactions are expected between this aphid species and poplar genotypes. Individuals of *M. persicae* originated from a monoclonal colony established from an apterous parthenogenetic female collected in 1999 on a potato plant in Loos-en-Gohelle (France). The colony was maintained under the same controlled conditions as *P. passerinii*, on turnips (Vilmorin).

For the protoplasts production, stem-cuttings of two *P. x canadensis* genotypes commonly planted in France, I-214 and Koster, were used for the experiments. I-214 is highly susceptible to *P. passerinii*, whereas aphids cannot settle on Koster which is consequently considered to be highly resistant to *P. passerinii* (Sallé et al., 2017). Consequently, compatible and incompatible interactions are expected between *P. passerinii* and I-214 and Koster, respectively, and non-host interactions should take place between *M. persicae* and both poplar genotypes. Stem cuttings (ca. 25 cm long, 2 cm diameter) were provided by the experimental nursery of Guéméné-Penfao (France). They were collected in the autumn of 2016, and kept at 2°C, in dry conditions until use. In January 2017, the stem-cuttings were removed from storage and planted in 0.4 L pots, filled with a sterile sand-compost (50:50) mixture (Klasmann substrate 4 no. 267). The cuttings were then transferred to a growth chamber (20 ± 1°C, 70 ± 10% relative humidity, 16/8 h light/dark photoperiod, 2.65 kLx, and watered three times a week).

For *in planta* functional validation of the effects of salivary proteins, two *Arabidopsis thaliana* (L.) Heynh. transgenic lines were used, the auxin-responsive reporter *pIAA2*::GUS (Bishopp et al., 2011) and the cytokinins-responsive reporter *pARR16*::GUS (European Arabidopsis Stock Centre). Seeds were sterilized

with chloral gas, sown in Petri dishes on 0.8% (w/v) agar with 1% (w/v) sucrose-containing 0.5 Murashige and Skoog medium (MS), stored for 2 days at 4°C, and grown on vertically oriented plates in growth chambers under a 16/8 h light/dark photoperiod at 18°C.

2.2. Salivary transcriptome

2.2.1. Sample collection, RNA isolation and *de novo* transcriptome assembly

About 500 adults of apterous parthenogenetic *P. passerinii* aphids were dissected to collect pairs of salivary glands. Total RNA was extracted using the GeneJET RNA Purification kit (Thermo Fischer Scientific), according to manufacturer's instructions. RNA was DNase treated using RNase-Free DNase Set (Qiagen). RNA concentration was measured using the Qubit® RNA Assay Kit (Life Technologies) and a Qubit® 2.0 Fluorometer (Invitrogen). Construction of cDNA-library and sequencing were performed by Eurofins® Genomics using a MiSeq v3 Reagent Kit (600 Cycles PE, Illumina, USA) and a MiSeq sequencer (Illumina). For the *de novo* transcriptome assembly, 15,453,942 pair-ended reads were sequenced and assembled using Velvet (v1.2.10; Zerbino & Birney, 2008) and Oases (v0.2.8; Schulz, Zerbino, Vingron & Birney, 2012) software tools (table S1). A multi-kmer approach was applied. Separate assemblies with different kmer lengths have been conducted and the individual assemblies have been merged to a final assembly. Kmer lengths of 69, 89, 109 and 129 were used. The separate assemblies were merged following the filter1-CD-HIT-EST procedure proposed in Yang & Smith (2013). This Transcriptome Shotgun Assembly project has been deposited at DDBJ/EMBL/GenBank under the accession GHDF00000000. The version described in this paper is the first version, GHDF01000000.

2.2.2. Annotation, secreted proteins detection and identification

To perform comparisons with *M. persicae* the transcriptome of this aphid was retrieved on NCBI (http://www.ncbi.nlm.nih.gov/genbank/, accession numbers: DW010205 - DW015017, EC387039 -

156 EC390992, EE570018 - EE572264, EE260858 - EE265165, ES444641 - ES444705, ES217505 - ES226848,
157 and ES449829 - ES451794). Salivary transcriptomes have been annotated using the pipeline described in
158 figure S1. Transcripts were first translated into amino acid sequences using Prodigal (v2.5; Hyatt et al.
159 2010). We then used the SignalP 4.0 Server (v4.1) to predict the presence of signal peptides and cleavage
160 sites in the amino acid sequences (Petersen, Brunak, von Heijne & Nielsen, 2011). To predict
161 transmembrane domains, we submitted each amino acid sequence with a signal peptide to the TMHMM
162 Server (v. 2.0; Ji et al., 2013). Putative proteins with a signal peptide and no transmembrane domain
163 were considered to be potential secreted proteins. The sequences of complete ORFs without signal
164 peptide were analyzed again with SecretomeP (v2.0; Bendtsen, Jensen, Blom, von Heijne & Brunak,
165 2004). To remove mitochondrial proteins with a signal peptide, which are not secreted in the saliva,
166 sequences were analyzed with TargetP (v1.1; Emanuelsson, Nielsen, Brunak, & von Heijne, 2000).
167 Likewise, to remove proteins of the endoplasmic reticulum with a signal peptide, sequences were
168 analyzed with PS-scan (Prosite pattern: PS00014), and with PredGPI (Pierleoni, Martelli & Casadio, 2008)
169 for glycosylphosphatidylinositol-anchor signals.
170 The remaining proteins were first mapped against the non-redundant protein sequences (nr) using
171 Blastp (v2.3.0, NCBI, accessed on 03/30/2016), with an E-value cutoff at 1^{e-3}. Protein domains were
172 annotated with Blast2Go (v3.3; Conesa et al., 2005), and InterProScan (v5.30-69; Jones et al., 2014).
173 Whenever possible, protein sequences were assigned to Gene ontology (GO) terms with an E-value
174 cutoff at 1^{e-6}, enzyme codes (EC) and KEGG pathways.
175 OrthoVenn (http://aegilops.wheat.ucdavis.edu/OrthoVenn; Wang et al., 2015) has been used to identify
176 orthologous proteins within and between salivary transcriptomes of the two aphids. Intraspecific
177 orthologous proteins are first grouped into clusters, which are then compared between species. Each
178 cluster has been annotated with the Uniprot database (http://www.uniprot.org; Pundir, Martin &
179 O'Donovan, 2017) and the nr peptide sequence database (NCBI, accessed on 03/30/2016).

To detect proteins orthologous to salivary effectors of aphids, protein sequences of known aphid effectors, i.e. C002, ACE1, ACE2, ACYPI39568, ACYPI00346, MpC002, Mp1, Mp2, Mp42, Mp55, Me10, Me23 (Guo et al., 2014; Jaouannet et al., 2014; Pan, Zhu, Luo, Kang & Cui, 2015), have been compared to the salivary transcriptome of *P. passerinii* with Blastp (E-value ≤ 1^{e-3}).

2.3. Functional validation assays

2.3.1. Aphid saliva collection

Aphids secrete two types of saliva within their host-plants, liquid and solid saliva (Will, Steckbauer, Hardt & van Bel, 2012). The solid saliva is secreted during probing. It hardens rapidly and forms a solid sheath encasing aphid stylets within the host-plant, while the liquid saliva is secreted within cells and sieve tubes (Will et al., 2012). Both types of saliva contain effectors (e.g. Will et al., 2012; Elzinga & Jander, 2013), and have been collected in our experiments. Because of the particular trophic substrates of *M. persicae* and *P. passerinii* (i.e. sap and galled tissues, respectively), a special protocol has been used for each species. The saliva of *P. passerinii* was collected after incubation of 30 to 40 individuals of 2^{nd} and 3^{rd} instars aphids on sachets of Parafilm© membranes containing an artificial diet (Cherqui & Tjallingii, 2000). The artificial diets were constituted by a disc of 0.5% (w/v) agar completed with 150 µL of 15% (w/v) sucrose. The saliva of *M. persicae* was collected after incubation of 30 to 40 individuals, of 3^{rd} and 4^{th} instars, on artificial diet containing 120 µL of a 15% (w/v) sucrose as previously described by Cherqui & Tjallingii (2000). Aphids were deposited in a feeding chamber during 24 h at 20°C, 60 ± 1% relative humidity and a 16/8 h light/dark period with 2.65 kLx. Feeding chambers containing the artificial diets, incubated in the absence of aphids, were used as control samples.

For *P. passerinii*, after 24 h aphid salivation, artificial diet discs were collected and transferred into 100 µL of TE buffer (10 mM Tris, 1 mM EDTA, pH 8). The salivary proteins were released from the artificial diet according to Yang et al. (2010), with slight modifications. The tubes containing artificial diet discs

were frozen in liquid nitrogen for 1 min, immediately thawed at 70°C for 3 min and then centrifuged at 11,000 x *g* for 20 sec. To discard the excess of agar, salivary extracts were centrifuged in Sartorius tubes with filters of 0.22 µm. The supernatant containing salivary proteins of *P. passerinii* were collected, pooled and then stored at -20°C. For *M. persicae,* after 24 h salivation, aphid saliva was collected according to Harmel et al. (2008). The artificial diet is collected containing soluble saliva. The solid saliva was collected during the rinsing of each lower Parafilm membrane with TE buffer containing 0.1% (w/v) of Tween 20 (TE/Tween). The extracts were centrifuged at 10,000 x *g* for 15 min. The salivary proteins in the pellet were collected, pooled with the soluble saliva and then stored at -20°C.

The sample containing protein saliva extracts were concentrated using 2 mL Vivaspin© tube (Sartorius) with 3kDa cut-off. The tubes were then centrifuged at 5,000 x *g* for 70 to 120 min according to sample volumes, and proteins adhering to membranes were recovered by 100 µL of TE/Tween buffer. Control samples were prepared with artificial diets from feeding chambers without aphids. The protein quantification was performed by measuring absorbance at 280 nm with the NanoDrop© 1000 (ThermoScientific).

2.3.2. Enzyme activities

Several enzyme substrates were added to the previously described artificial diets with or without agarose to detect enzymatic activities present in saliva excreted from the aphid. To visualize proteins in the salivary sheaths, the lower Parafilm© membranes were stained by adding a drop of 0.01% (w/v) Coomassie blue in 10% (v/v) glycerol for 2 h. Dihydroxyphenylalanine (DOPA), 0.1% (w/v) was added to identify phenoloxidase activity (PO; catechol oxidase, EC 1.10.3.1). The enzymatic product, melanin, should stain salivary sheaths and halos around the sheaths. To detect peroxidase (EC 1.11.1.7) activity, artificial diets were immersed for some minutes in 0.1% (w/v) diaminobenzidine (DAB, Sigma) in 50 mM Tris (pH 7.5) containing 0.1% (v/v) H_2O_2 (Sigma). The enzymatic product should induce reddish staining of

228 salivary sheaths and halos. For identification of pectinase activity, 0.1% (w/v) of pectin (Sigma) was
229 added to the medium. After exposure to aphids, the gel was transferred for 3 h into a Petri dish
230 containing 50 mM citrate-phosphate buffer, at pH 5.0 to detect pectin (methyl) esterase (PME, EC
231 3.1.1.11) and at pH 6.4 to detect polygalacturonase (PG, EC 3.1.1.15). The gel was then stained with a
232 solution of 0.01% (w/v) ruthenium red (Sigma) for 1 h, and then washed several times with distilled
233 water. At pH 6.4, red halos around the salivary sheaths indicate PME activity, while non-staining halos at
234 pH 5 in the pink pectin indicate PG activity. Finally, for proteinase activity (EC 3.4.99), 0.5% (w/v) of
235 gelatin (Sigma) was added to the medium. After exposure to aphids, the medium was incubated
236 overnight in a solution of 50 mM Tris (pH 8) containing 100 mM NaCl and 10 mM $CaCl_2$, then stained with
237 Coomassie blue. An absence of blue staining shows proteinase activity. All observations of proteins and
238 enzymatic activities were performed by light microscopy (Axioplan 2, Zeiss, Jena, Germany).
239

240 ### 2.3.3. Poplar protoplast preparations and treatments

241 Mesophyll protoplasts of the two poplar genotypes were obtained from young leaves as described in Wu
242 et al. (2009). Leaves were cut into 1–2 mm fine strips in 0.3 M sorbitol and 66.67 mM $CaCl_2$ (pH 5.6) and
243 lysed in an enzyme solution (0.6 M mannitol, 0.25% (w/v) cellulase Onozuka R-10, 0.05% (w/v)
244 macerozyme R-10) in the dark for 16 h with gentle shaking (30 rpm) at room temperature. Protoplasts
245 were collected by filtering the lysis solution through a 70 µm cell strainer (Falcon®) and concentrated by
246 spinning down at ≈ 800 x *g* for 10 min at 4 °C. The pellet was washed twice with W5 buffer (154 mM
247 NaCl, 125 mM $CaCl_2$, 5 mM KCl, 5 mM glucose, 0.03% (w/v) MES, pH 5.8) and then resuspended in 0.6 M
248 mannitol to a final concentration of 1×10^6 protoplasts per mL. Protoplasts (1.10^6) were incubated at
249 20°C with gentle shaking (40 rpm) for 3 h with aphid salivary proteins or with protein extraction buffer
250 (control). Preliminary experiments investigating expression of 10 poplar genes, and conducted with 1,
251 10, 20, 40 or 80 µg of salivary proteins, indicated that the optimal response (i.e. the maximum fold

252 change) was observed with 1 and 10 µg of salivary proteins of *P. passerinii* and *M. persicae*, respectively.
253 Protoplast viability, before and after treatment with aphid saliva, was assessed using 0.005% (w/v)
254 fluorescein diacetate (FDA). After 5 min of incubation protoplasts were observed under blue light
255 epifluorescence, and cell viability was estimated as the percentage of fluorescent cells. Most protoplasts
256 were intact and viable after enzymatic digestion with cellulase and macerozyme (98%), as well as after
257 incubation with salivary proteins (95%; Fig. S2).
258
259 ### 2.3.4. Quantitative RT-PCR
260 After the aphid saliva treatments, protoplasts were centrifuged at ≈ 800 x *g* for 2 min. Total RNAs were
261 extracted with the RNeasy® Plant Kit Mini Kit (Qiagen). A DNase treatment with the RNase-free DNase
262 Set (Qiagen) was carried out for 15 min at 25°C. Total RNA concentration was determined using a
263 Nanodrop ND-1000 spectrophotometer. All RNA samples were rejected if they did not reach a minimum
264 concentration of 100 ng μL^{-1}, a 260 nm/280 nm ratio between 1.8 and 2.0. Poly(dT) cDNA was prepared
265 from 1 µg total RNA using the iScriptTMcDNA Synthesis Kit (Bio-Rad) and quantified with a LightCycler
266 480 (Roche) and SYBR GREEN I Master (Roche), according to the manufacturer's instructions. PCR was
267 carried out in 384-well optical reaction plates heated for 10 min to 95°C to activate hot start Taq DNA
268 polymerase, followed by 40 cycles of denaturation for 60 sec at 95°C and annealing/extension for 60 sec
269 at 58°C. The distribution of the quantitative RT-PCR mix containing SYBR Green I Master (Roche), cDNAs
270 and primers was performed using the EVO150© (Tecan) pipetting robot in a 384-well plate. The
271 expression of 43 genes, belonging to eight different physiological processes or metabolic pathways (i.e.
272 auxin, cytokinins, jasmonates, ethylene, salicylic acid, phenolic compounds, reactive oxygen species
273 (ROS), cell cycle), was quantified with specific primer pairs designed by Quant-Prime (Arvidsson,
274 Kwasniewski, Riaño-Pachón & Mueller-Roeber, 2008) based on the *Populus trichocharpa* sequence (v3.0)
275 from Phytozome (https://phytozome.jgi.doe.gov/pz/portal.html; Table S2). Expression levels were

normalized to the levels of *PtUBIQUITIN10* (*PtUBQ10*), commonly used as a reference gene in plants (e.g. Tong, Gao, Wang, Zhou & Zhang, 2009). All RT-qPCR experiments were done with three independent biological replicates, with two technical replicates each. One of the biological replicates of the *M. persicae* – Koster interaction has been excluded from the analyses because of technical issues during quantification. Relative gene expression was calculated according to the $^{\Delta\Delta}$Cp method, with protoplasts incubated with protein extraction buffer as controls. Primers used for gene expression analysis are listed in Table S2.

2.3.5. Histochemical analysis of GUS activity

Transgenic seedlings of *A. thaliana* (five-day-old and eight-day-old for *pIAA2*::GUS and *pARR16*::GUS, respectively) were incubated with 2 mL of liquid MS containing 1 µg and 10 µg of aphid salivary proteins (in TE/Tween buffer) of either *P. passerinii* or *M. persicae* for 3 h and 4 h for *pIAA2*::GUS and *pARR16*::GUS, respectively. Positive controls were incubated with 20 µM of indole acetic acid (IAA) (Sigma-Aldrich), and 20 µM of 6-benzylaminopurine (BAP) (Sigma-Aldrich). Negative controls were incubated in liquid MS and corresponding volumes of TE/Tween buffer. Five seedlings were used for each modality. Seedlings were then incubated in reaction buffer containing 0.1 M sodium phosphate buffer (pH 7), 2 mM ferricyanide, 2 mM ferrocyanide, 0.1% (v/v) Triton X-100 and 1 mg ml^{-1} X-Gluc for 1 up to 24 h in dark at 37 °C. Afterwards, chlorophyll was removed by destaining in 70% ethanol and seedlings were cleared as described by Malamy and Benfey (1997). GUS expression was monitored by differential interference contrast microscopy.

2.4. Data analysis

All tests were carried out with the statistical software R 2.11.0 (R Development Core Team, 2013). RT-qPCR results have been expressed as fold-changes in gene expression compared to the reference gene

300 *PtUBQ10*. Fold-changes have been $\log_2$ - transformed. Following this transformation, fold-changes varied
301 between -∞ and +∞, with negative values corresponding to gene underexpression, positive values to
302 overexpression and zero, to no change in gene expression. Permutational multivariate anovas
303 (permanovas), using 1000 permutations, were computed to test the effect of aphid species and host
304 plant genotype on the simultaneous fold-changes in gene expression of the 43 considered poplar genes
305 using the R package vegan (Oksanen et al. 2013). To visualize similarities and differences in fold-changes
306 a heatmap was built, with genes in columns and modalities in lines. The heatmap was built with a Z-
307 score, i.e. $\log_2$ – transformed fold changes which have been normalized and centered per column.
308 Hierarchical clustering with Euclidean distances was added to the heatmap to visualize the proximity
309 among genes in columns and among modalities in lines.
310 A univariate model has also been used to analyze the effect of modalities (i.e. aphid species and host
311 genotype) on fold-changes of each gene. The model equation was:

$$\log_{10}(y_{ij}) = \alpha_i + \varepsilon_{ij}$$

312 where y_{ij} is the fold-change for the modality i and the biological replicate j, and α_i is the effect of the
313 modality i on relative gene expression. The model error follows a normal distribution, with a null mean
314 and a variance σ^2. There is no intercept in this model and 4 independent α_i parameters were estimated,
315 corresponding to each aphid – poplar genotype combination. These parameters were estimated with a
316 Bayesian approach, with $\alpha_i \sim N(0, 0.5^2)$ for prior. The parameters have been estimated with a Markov
317 Chain Monte Carlo algorithm and the package R brms (Buerkner, 2016). The maxima *a posteriori* and
318 95% credibility intervals were calculated, with downregulation and upregulation probabilities for each
319 gene. A credibility interval excluding 1 (i.e. the constitutive expression of genes) indicates a significant
320 effect of aphid saliva on gene expression. This approach was selected because it allows to perform
321 statistical analyses with a limited number of biological replications.
322

323 ## 3. Results

324 ### 3.1. Annotation, secreted proteins detection and identification

325 From 36,312 and 3,233 transcripts, 1,243 and 221 transcripts were predicted to encode for secreted
326 salivary proteins in *P. passerinii* and *M. persicae*, respectively. About half of them (604) have been
327 annotated for *P. passerinii* and 190 for *M. persicae*. Using OrthoVenn, 121 and 58 protein clusters have
328 been identified for *P. passerinii* and *M. persicae*, respectively. About 17% of these clusters were common
329 between the two aphids (Table S3).
330 Blast2GO determined that *P. passerinii* salivary proteins were predominantly binding proteins and
331 enzymes (Fig. 1, table S4). The most common enzymes were peptidases (especially serine-type and
332 cysteine-type endopeptidases), kinases (especially phosphatidylinositol phosphate (PIP) kinases) and
333 hydrolases. Several enzymes involved in the degradation of carbohydrates (i.e. cellulase, trehalase, β-
334 glucuronidase, mannosidase and glucosylceramidase), and of phenolic compounds (i.e. peroxidase and
335 oxidoreductase) were also identified (Fig. 1, table S4). Among binding proteins, dimerization protein,
336 nucleic acids binding (especially DNA binding), nucleotide binding (especially ATP binding) and cation-
337 binding (mostly calcium ion-binding and zinc-binding proteins) were the most commonly found (Fig. 1,
338 table S4). Proteins related to hormone activity were also identified. Glucose dehydrogenases were also
339 detected with OrthoVenn (table S3). Among the 12 aphid salivary effectors considered, five were
340 identified in *P. passerinii*, with low E-values (< 7 e^{-71}): Mp10, ARMET, ACE 1, ACE2 and ACE3.
341

342 ### 3.2. Enzyme activities

343 Staining with Coomassie blue confirmed the protein nature of the salivary sheath material (Fig. 2A) and
344 DOPA staining indicated a phenoloxidase activity in the sheaths (Fig. 2B). Black halos were also observed
345 around some sheaths (Fig. 2B). Likewise, peroxidase activity was found in salivary sheaths and halos

346 around sheaths (Fig. 2C). However, no pectinesterase, polygalacturonase and proteinase activity was
347 detected.
348
349 ### 3.3. Quantitative RT-PCR
350 The multivariate analysis based on the expression of the 43 genes showed a highly significant effect of
351 aphid species (pseudo-$F_{1, 10}$ = 12.07, P < 0.001), no effect of poplar genotype, but a significant aphid x
352 poplar genotype interaction (pseudo-$F_{1, 10}$ = 3.51, P = 0.038). This indicated that the salivary proteins
353 effect differed depending on aphid x poplar genotypes combinations. Fold changes across modalities are
354 presented in figure 3. The hierarchical clustering of modalities (left dendrogram) shows an arrangement
355 of modalities into two groups. In the upper group, most poplar genes were upregulated following
356 incubation with salivary proteins, while in lower group most genes were downregulated (Fig. 3). The
357 upper group gathered most biological replicates of incompatible (i.e. *P. passerinii* – Koster) and non-host
358 (i.e. *M. persicae* – Koster, *M. persicae* – I-214) interactions. The lower group gathered all replicates of
359 compatible interactions (i.e. *P. passerinii* – I-214) and an incompatible one. The hierarchical clustering of
360 genes (upper dendrogram) showed that genes could also be arranged into two groups. The group on the
361 left allowed to separate the effect of salivary proteins of *M. persicae*, with a general downregulation of
362 genes, from those of *P. passerinii*, with a general upregulation (Fig. 3). The group on the right allowed to
363 separate compatible interactions, with a general downregulation of genes, from other interactions
364 during which genes were generally upregulated (Fig. 3). There was no clustering of genes according to
365 physiological process or metabolic pathway.
366 For the auxin pathway, the compatible interaction was characterized by a downregulation of genes
367 related to auxin transport (i.e. *PtAUX1* and *PtPIN1* with downregulation probabilities of 62% and 86%,
368 respectively) and homeostasis (i.e. *GH3* with a downregulation probability >99%; Fig. 4A). However,
369 there was no effect on genes involved in auxin biosynthesis (i.e. *PtNIT1* and *PtYUCCA*). Reverse variations

were observed for non-host and incompatible interactions which led to an upregulation of *PtGH3*, with upregulation probabilities >99% for *M. persicae* and 86% for *P. passerinii*, and upregulations of genes related to auxin transport with probabilities always higher than 86% (Fig. 4A).

For the cytokinin pathway, the compatible interaction did not affect the expression of genes related to cytokinin metabolism (i.e. *PtLOG5* and *PtIPT*), but downregulated cytokinin signaling genes (*PtAHK4* and *PtARR2*), with downregulation probabilities >99% (Fig. 4B). Non-host interactions led to upregulations of all genes but *PtLOG5*, with probabilities >95% (Fig. 4B). Response of genes to the incompatible interaction followed a similar trend, with upregulation of all genes, including *PtLOG5*, with probabilities >95%.

Regarding biotic stress signaling (i.e. jasmonates, salicylic acid, ethylene and ROS), the compatible interaction was characterized by null or downregulation responses for all the considered genes (Fig. S3). For ROS genes weak downregulations were also observed for non-host interactions (>85% and >64% downregulation probabilities for *PtSOD* and *PtCAT*, respectively) and a weak upregulation for the incompatible interaction (91% and 77% upregulation probabilities for *PtSOD* and *PtCAT*, respectively). For salicylic acid, jasmonates and ethylene, non-host interactions induced a strong upregulation of most genes (>99% upregulation probabilities in most cases), except *PtPR5* for salicylic acid which was downregulated (>98% downregulation probabilities), *PtAOS* for jasmonates and *PtEIN2* for ethylene which did not respond. The incompatible interaction resulted in an upregulation of all genes involved in jasmonates and ethylene pathways but to a lesser extent than non-host interactions (>81% upregulation probabilities), except *PtJAZ1* which was downregulated (73% downregulation probability) and *PtJAR1*, *PtERF1* which were not affected. For salicylic acid, weak upregulations were observed for *PtNPR1*, *PtPR5* and *PtNDR1* (>62% upregulation probabilities), and no effect was detected for *PtPR1* and *PtEDS1*.

For genes involved in the phenolic compounds pathway, *PtF5H* and *PtANT* were downregulated during the compatible interaction (>85% downregulation probability), while all genes were upregulated during

394 non-host and incompatible interactions (>89% upregulation probability in all cases; Fig. S3). Finally,
395 regarding genes involved in cell cycle, *PtCYCD5*, *PtMCM2* and *PtRBR* tended to be downregulated during
396 compatible interactions (>72% downregulation probability). Conversely, most genes, except *PtCAK1* and
397 *PtMCM2*, were upregulated during non-host interactions (>94% upregulation probabilities in most
398 cases), and most genes were not affected during incompatible interactions, except *PtCDK5*, *PtCDK20* and
399 *PtCAK1* which were upregulated (>95% upregulation probabilities; Fig. S3).
400

401 ### 3.4. Histochemical analysis of GUS activity

402 Salivary proteins of *P. passerinii* increased *pIAA2*::GUS signals (Fig. 5E, 5F, 5I, 5J), which were similar to
403 those caused by an exogenous application of auxin (Fig. 5A and 5B). Incubation with salivary proteins of
404 *M. persicae* resulted in faint colorations (Fig. 5G, 5H, 5K, 5L), similar to those of negative controls (Fig. 5C
405 and 5D).
406 Positive controls of *pARR16*::GUS were characterized by a strong staining in the middle part of root
407 central cylinder (Fig. 6A and 6B), which was weak in negative controls as well as with *M. persicae* salivary
408 proteins (Fig. 6G, 6H, 6K, and 6L). No coloration was visible in the roots of seedlings incubated with
409 salivary proteins of *P. passerinii* (Fig. 6E, 6F, 6I and 6J).
410

411 ## 4. Discussion

412 Plant manipulation by parasites requires a finely tuned reprogramming of host metabolism, achieved
413 through secretion of effectors into the host plant (Hogenhout & Bos, 2011; Giron et al., 2016). Using
414 both *in vivo* and *in planta* approaches, we confirmed that salivary proteins impact gene transcription of
415 its host tree, strongly suggesting they mediate the interactions between *P. passerinii* and its host-tree.
416 Salivary extracts of *P. passerinii* significantly affected gene expression of the two host-plant genotypes
417 considered, in a markedly different way. Compatible interactions were characterized by a general trend

418 of gene downregulation in all the metabolic pathways and physiological processes investigated, including
419 genes involved in biotic stress signaling. This supports the hypothesis that the saliva of *P. passerinii*
420 includes effectors proteins affecting plant signaling and defense mechanisms.
421
422 Several of the detected salivary proteins may interfere with plant signaling. PIP kinases were quite
423 common in the saliva of *P. passerinii*, but have not been previously reported from any aphid saliva. These
424 enzymes catalyze phosphorylation of phosphatidyl-inositol into phosphatidylinositol-4-5-biphosphate
425 (PIP_2). Hydrolysis of PIP_2 produces secondary messengers like diacylglycerol and inositol-1-4-5-
426 triphosphate (IP_3), which can in turn be hydrolyzed into phosphatidic acid (PA), considered an important
427 signaling molecule in plants, triggered in response to various biotic and abiotic stresses (Testerink &
428 Munnik, 2005). Likewise, PIP_2 and IP_3 can affect cellular oscillations of Ca^{2+} and are involved in multiple
429 processes including cell cycle and phytohormone regulation (Xue, Chen & Mei, 2009). Other proteins,
430 frequently detected in the saliva of *P. passerinii*, may also interfere with secondary messengers like
431 calcium-binding, ATP-binding, and GTP-binding proteins or with hormone signaling like hormone-binding
432 proteins (Vandermoten et al., 2014; Giron et al., 2016). Likewise, it has been hypothesized that trehalase
433 may interfere with trehalose-based defense responses in *A. thaliana* (Nicholson et al., 2012), and
434 cellulases may also contribute to the degradation of oligogalacturonides involved in damage signaling
435 pathways (Cherqui & Tjallingii, 2000). Nucleic acid-binding proteins and protein-binding proteins could
436 also participate in the manipulation of host-plant metabolism (Vandermoten et al., 2014). Finally,
437 oxidoreductases, especially peroxidases and phenoloxidases could degrade phenolic compounds of the
438 host plant (Cherqui & Tjallingii, 2000; Carolan, Fitzroy, Ashton, Douglas & Wilkinson, 2009). Gall
439 induction by *P. passerinii* in susceptible host genotypes is characterized by transient accumulation of
440 phenolic compounds (Dardeau et al., 2014), and oxidoreductases could help aphids to cope with these

441 secondary metabolites. Glucose dehydrogenases may similarly help aphids to detoxify defensive
442 compounds of the host-plant (Carolan et al., 2011; Nicholson et al., 2012).
443 Several proteins orthologous to salivary effectors of *M. persicae* and *A. pisum* have been identified.
444 Likewise, many of the proteins detected in our study (e.g. calcium-binding, DNA-binding, ATP-binding,
445 GTP-binding proteins, glucose dehydrogenases, oxidoreductases, trehalases and phosphatases) have also
446 been previously identified in the saliva of different aphid species, which were not gall-inducers (Harmel
447 et al., 2008; Nicholson et al., 2012; Elzinga & Jander, 2013; Vandermoten et al., 2014). Therefore,
448 although these proteins probably contribute to plant manipulation by aphids (Elzinga & Jander, 2013),
449 they are probably not specifically involved in gall induction. Interestingly, calcium-binding proteins are
450 supposedly key components of sap-feeding aphids' saliva, preventing the plugging of sieve tubes (Will et
451 al., 2007). Since *P. passerinii* does not feed on sap (Pointeau et al., 2012), it suggests that these proteins
452 also play other crucial roles during aphid-plant interactions. Several proteins detected in the saliva of *P.*
453 *passerinii* such as serine proteases, acid phosphatases, lipases and metalloproteases have been proposed
454 as potential effectors involved in formation and/or maintenance of fig wasps galls (Martinson, Hackett,
455 Machado & Arnold, 2015).
456 *In situ* biochemical assays confirmed the presence of peroxidases in both solid and soluble saliva of *P.*
457 *passerinii*. The phenoloxidase activity is also congruent with the numerous oxidoreductase sequences
458 identified in the salivary transcriptome. Likewise, the absence of pectin (methyl) esterase and
459 polygalacturonase activity during *in situ* bioassays is consistent with their absence in the salivary
460 transcriptome. However, while numerous proteases were identified among the salivary proteins of *P.*
461 *passerin*ii, no activity was observed during *in situ* bioassays. Gelatin was probably not the adequate
462 substrate to detect the protease activity of *P. passerinii*. Additional *in situ* assays could be conducted to
463 detect, in *P. passerinii* saliva, the activity of the proteases and possibly other enzymes like cellulases

(Cherqui & Tjallingii, 2000). A proteomic analysis of salivary extracts should also confirm and complement the predictions of our transcriptomic approach (Carolan et al., 2011; Boulain et al., 2018).

To knock-down or divert stress signaling and/or ensure finely-tuned reprogramming of host metabolism and anatomical transformation of host tissues, plant manipulation by herbivores or pathogens generally requires reconfiguration of phytohormone pathways and signaling (Giron, Frago, Glevarec, Pieterse & Dicke, 2013; Tooker & Helms, 2014). Both RT-qPCR experiments and histochemical assays confirmed that *P. passerinii* can actively manipulate phytohormone pathways during compatible interactions. This is in line with the numerous proteins potentially interfering with plant signaling and metabolism found in the aphid saliva. Salivary extracts of *P. passerinii* did not affect the auxin biosynthesis during compatible interactions, but downregulated auxin transporter genes such as *PtPIN1* and *PtAUX1*, as well as *PtGH3*, which is involved in the homeostasis of auxin active forms (Park et al., 2007). These downregulations could lead to intracellular accumulation of active auxin forms, and result in the targeted cell hypertrophy and multiplication commonly observed during gall differentiation by *P. passerinii* (Dardeau et al., 2014). The activation of the auxin-responsive promoter *IAA2* during *in planta* assays with transgenic seedlings of *A. thaliana* further supports this hypothesis of an intracellular accumulation of auxin during gall initiation by *P. passerinii*. Similar auxin accumulation, as a result of a reduction in both *PtGH3* activity and auxin transport, is also probably involved in the initiation and development of root galls by cyst and root-knot nematodes (Karczmarek, Overmars, Helder & Goverse, 2004), suggesting a potentially convergent manipulation strategy between these organisms. As genes related to cytokinin biosynthesis (*PtIPT*) and activation (*PtLOG5*) were not affected by salivary proteins of *P. passerinii*, the strong downregulation of cytokinin signaling genes (*PtAHK4*, *PtARR2* and *PtARR16*) upon treatment could correspond to an auxin accumulation-induced regulation loop (Jones et al., 2010; Schaller, Bishopp, & Kieber, 2015). In this aspect, *P. passerinii* could manipulate auxin and cytokinin plant responses to promote the host division

cycle leading to the formation of galls (Giron et al., 2013), which provide to the insects food and shelter at the expense of the host plant (Tooker & De Moraes, 2008).

Apart from the Mp10 effector, the saliva of *P. passerinii* and *M. persicae* shared few similarities. The transcriptomes of *P. passerinii* and *M. persicae* have been obtained with a different sequencing and assembly methods (Ramsay et al., 2007). This probably explains the difference in transcripts amounts gathered for both aphids and several salivary proteins of *M. persicae* might be missing in its transcriptome, leading to an apparently low similarity between secretomes. Previous comparisons among salivary proteins of aphid species also indicated that aphids with different host species and / or feeding strategies exhibited very different salivary protein profiles (Cooper, Dillwith & Puterka, 2011; Vandermoten et al., 2014). This is in agreement with the highly significant effect of aphid species on gene expression profiles in both poplar genotypes. Nonetheless, gene expression profiles of poplar protoplasts during incompatible interactions shared many similarities with those observed during non-host interactions. Both types of interactions were characterized by an overall upregulation of host genes, which was generally more important during non-host interactions than during incompatible ones, probably because one of the three biological replicates of incompatible interactions shared similarities with compatible interactions. During both non-host and incompatible interactions, most genes involved in jasmonates, ethylene and salicylic acid pathways were upregulated. All of these pathways can be activated following aphid feeding, together or separately, depending on the aphid – plant interaction system considered (Morkunas, Mai & Gabryś, 2011; Kerchev, Fenton, Foyer & Hancock, 2012; Louis & Shah, 2013). Due to the salicylic acid - jasmonates cross-talk, a differential gene expression between the two pathways could be expected (Zarate, Kempema & Walling, 2007), but was not observed here. However, this may occur later during the interaction, since in our experiments we only considered early gene responses (Kerchev et al., 2012). As a consequence of activation of plant defense signaling, genes

related to secondary metabolism, i.e. *PtF3'5'H, PtANT* and *PtF5H* were also upregulated during both incompatible and non-host interactions, while they were unaffected or downregulated during compatible interactions. This is in agreement with previous histochemical analyses showing a light and transient accumulation of phenolic compounds followed by their marked disappearance in galled tissues during a compatible interaction, while their accumulation was strong and continuous during an incompatible interaction (Dardeau et al., 2014).

Interestingly, most of the few genes that were differentially expressed during non-host and incompatible interactions were related to biotic stress signaling, and all genes but *PtJAZ1* were upregulated during incompatible interactions while they were unaffected or downregulated during non-host interactions. These genes included ROS-related genes, *PtSOD* and *PtCAT*, the expression of which was slightly downregulated during non-host interactions. A similar repression of *SOD* and *CAT* genes, leading to an increase in H_2O_2 content, together with an upregulation of *JAZ1* and *PR1*, has been reported in potato leaves infested by *M. persicae* (Kerchev et al., 2012). Some phytohormones-related genes were also upregulated during incompatible interactions only, like *PtAOS* for jasmonates, *PtPR5* for salicylic acid, *PtLOG5* for cytokinins, *PtNIT1* for auxin, and finally *PtEIN2* for ethylene. This latter gene is involved in transduction of ethylene signaling and can be up- or downregulated during both compatible and incompatible interactions in different plant-aphid systems and plays equivocal roles during host-plant resistance to *M. persicae* (Morkunas et al., 2011; Louis & Shah, 2013). Moreover, the putative intracellular accumulation of auxin during compatible interactions could also interfere with salicylic acid signaling and defense responses (Park et al., 2007), which is congruent with the overall downregulation of salicylic acid pathway related genes. The downregulation of *PtAHK4* and *PtARR2* could also interfere with stress signaling by preventing both accumulation of jasmonates and activation of *PtPR1* (O'Brien & Benkova, 2013), which is consistent with our observations during compatible interactions. As a result,

535 the effectors of *P. passerinii* saliva, in addition to modifying phytohormonal contents, down-regulate the
536 plant defenses to allow gall formation.
537
538 In conclusion, our transcriptomic analysis of the saliva of *P. passerinii* and *M. persicae* showed that the
539 gall-inducing aphid probably secretes a highly peculiar saliva, filled with potential effectors that may
540 interfere with several plant secondary messengers and signaling pathways. Our *in vivo* and *in planta*
541 approaches confirmed the ability of salivary extracts of the gall-inducing insects to manipulate host
542 response during compatible interactions. As expected phytohormones pathways were strongly affected,
543 probably to impair biotic stress signaling but also to reconfigure host metabolism and anatomy. Although
544 the saliva of *P. passerinii* and *M. persicae* were very different, incompatible and non-host interactions led
545 to similar host responses, with a different intensity however, and few differences in biotic stress
546 signaling. Additional modalities including different populations of *P. passerinii*, different poplar
547 genotypes with intermediate resistance levels, leading for instance to semi-compatible interactions, and
548 additional host metabolic pathways could be considered in future experiments and give further insights
549 on the molecular processes underpinning failed and successful host manipulation by a gall-inducer.
550

551 ## 5. Acknowledgements

552 We thank Léa Fléchon for her assistance with transcriptome analyses. This study has been supported by
553 the Région Centre-Val de Loire Project no. 2014 00094521 (InsectEffect) coordinated by D. Giron.
554

6. References

Arvidsson S., Kwasniewski M., Riaño-Pachón D.M. & Mueller-Roeber B. (2008). QuantPrime--a flexible tool for reliable high-throughput primer design for quantitative PCR. *BMC Bioinformatics*, 9, 465.

Atamian H.S., Chaudhary R., Dal Cin V., Bao E., Girke T. & Kaloshian I. (2013) *In planta* expression or delivery of potato aphid *Macrosiphum euphorbiae* effectors Me10 and Me23 enhances aphid fecundity. *Molecular Plant-Microbe Interactions*, 26, 67–74.

Bendtsen J.D., Jensen L.J., Blom N., Von Heijne G. & Brunak, S. (2004). Feature-based prediction of non-classical and leaderless protein secretion. *Protein Engineering Design and Selection*, 17, 349-356.

Bishopp A., El-Showk S., Weijers D., Scheres B., Friml J., Benková E., … Helariutta Y. (2011). A mutually inhibitory interaction between auxin and cytokinin specifies vascular pattern in roots. *Current Biology*, 21, 917-926.

Boulain H., Legeai F., Guy E., Morlière S., Douglas N.E., Oh J., ... & Sugio A. (2018). Fast evolution and lineage-specific gene family expansions of aphid salivary effectors driven by interactions with host-plants. *Genome Biology and Evolution*, 10, 1554-1572.

Buerkner P.C. (2016) brms: An R package for Bayesian multilevel models using Stan. *Journal of Statistical Software*, 80, 1-28.

Carolan J.C., Fitzroy C.I.J., Ashton P.D., Douglas A.E. & Wilkinson T.L. (2009). The secreted salivary proteome of the pea aphid *Acyrthosiphon pisum* characterised by mass spectrometry. *Proteomics*, 9, 2457–2467.

Carolan J.C., Caragea D., Reardon K.T., Mutti N.S., Dittmer N., … Edwards O.R. (2011). Predicted effector molecules in the salivary secretome of the pea aphid (*Acyrthosiphon pisum*): a dual transcriptomic/proteomic approach. *Journal of Proteome Research*, 10, 1505–1518.

577 Chaudhary R., Atamian H.S., Shen Z., Briggs S.P. & Kaloshian I. (2014). GroEL from the endosymbiont
578 *Buchnera aphidicola* betrays the aphid by triggering plant defense. *Proceedings of the National Academy*
579 *of Sciences*, 111, 8919-8924.
580 Cherqui A. & Tjallingii W.F. (2000). Salivary proteins of aphids, a pilot study on identification, separation
581 and immunolocalisation. *Journal of Insect Physiology*, 46, 1177–1186.
582 Conesa A., Götz S., García-Gómez J.M., Terol J., Talón M. & Robles M. (2005). Blast2GO: a universal tool
583 for annotation, visualization and analysis in functional genomics research. *Bioinformatics*, 21, 3674–
584 3676.
585 Cooper W.R., Dillwith J.W. & Puterka G.J. (2011). Comparisons of salivary proteins from five aphid
586 (Hemiptera: Aphididae) species. *Environmental Entomology*, 40, 151-156.
587 Dardeau F., Deprost E., Laurans F., Lainé V., Lieutier F. & Sallé, A. (2014). Resistant poplar genotypes
588 inhibit pseudogall formation by the wooly poplar aphid, *Phloeomyzus passerinii* Sign. *Trees*, 28, 1007-
589 1019.
590 De Vos M. & Jander G. (2009). *Myzus persicae* (green peach aphid) salivary components induce defence
591 responses in *Arabidopsis thaliana*. *Plant Cell & Environment*, 32, 1548–1560.
592 Elzinga D.A. & Jander G. (2013). The role of protein effectors in plant–aphid interactions. *Current Opinion*
593 *in Plant Biology*, 16, 451-456.
594 Emanuelsson O., Nielsen H., Brunak S. & von Heijne G. (2000). Predicting subcellular localization of
595 proteins based on their N-terminal amino acid sequence. *Journal of Molecular Biology*, 300, 1005-1016.
596 Favery B., Quentin M., Jaubert-Possamai S. & Abad P. (2016). Gall-forming root-knot nematodes hijack
597 key plant cellular functions to induce multinucleate and hypertrophied feeding cells. *Journal of insect*
598 *physiology*, 84, 60-69.
599 Giron D., Frago E., Glevarec G., Pieterse C.M. & Dicke M. (2013). Cytokinins as key regulators in plant–
600 microbe–insect interactions: connecting plant growth and defence. *Functional Ecology*, 27, 599-609.

601 Giron D., Huguet E., Stone G.N. & Body M. (2016). Insect-induced effects on plants and possible effectors
602 used by galling and leaf-mining insects to manipulate their host-plant. *Journal of Insect Physiology*, 84,
603 70-89.
604 Guiguet A., Dubreuil G., Harris M.O., Appel H., Schultz J.C., Pereira M.H. & Giron D. (2016). Shared
605 weapons of blood- and plant-feeding insects: surprising commonalities for manipulating hosts. *Journal of*
606 *Insect Physiology*, 84, 4–21.
607 Guo K., Wang W., Luo L., Chen J., Guo Y. & Cui F. (2014). Characterization of an aphid-specific, cysteine-
608 rich protein enriched in salivary glands. *Biophysical Chemistry*, 189, 25–32.
609 Harmel N., Létocart E., Cherqui A., Giordanengo P., Mazzucchelli G., Guillonneau F., … Francis F. (2008).
610 Identification of aphid salivary proteins: a proteomic investigation of *Myzus persicae*. *Insect Molecular*
611 *Biology*, 17, 165–174.
612 Hogenhout S.A. & Bos J.I. (2011). Effector proteins that modulate plant–insect interactions. *Current*
613 *Opinion in Plant Biology*, 14, 422-428.
614 Hyatt D., Chen G.L., LoCascio P.F., Land M.L., Larimer F.W. & Hauser L.J. (2010). Prodigal: prokaryotic
615 gene recognition and translation initiation site identification. *BMC Bioinformatics*, 11:119.
616 Jaouannet M., Rodriguez P.A., Thorpe P., Lenoir C.J.G., MacLeod R., Escudero-Martinez C. & Bos J.I.B.
617 (2014). Plant immunity in plant–aphid interactions. *Frontiers in Plant Science*, 5, 663.
618 Ji R., Yu H., Fu Q., Chen H., Ye W., Li S. & Lou Y. (2013). Comparative transcriptome analysis of salivary
619 glands of two populations of rice brown planthopper, *Nilaparvata lugens*, that differ in virulence. *PloS*
620 *one*, 8, e79612.
621 Jones B., Gunnerås S.A., Petersson S.V., Tarkowski P., Graham N., May S., … Ljung, K. (2010). Cytokinin
622 regulation of auxin synthesis in *Arabidopsis* involves a homeostatic feedback loop regulated via auxin and
623 cytokinin signal transduction. *The Plant Cell*, 22, 2956-2969.

624 Jones P., Binns D., Chang H.Y., Fraser M., Li W., McAnulla C., ... Pesseat S. (2014). InterProScan 5:
625 genome-scale protein function classification. *Bioinformatics*, 30, 1236-1240.
626 Karczmarek A., Overmars H., Helder J. & Goverse A. (2004). Feeding cell development by cyst and
627 root-knot nematodes involves a similar early, local and transient activation of a specific auxin-inducible
628 promoter element. *Molecular Plant Pathology*, 5, 343-346.
629 Kerchev P.I., Fenton B., Foyer C.H. & Hancock R.D. (2012). Infestation of potato (*Solanum tuberosum* L.)
630 by the peach-potato aphid (*Myzus persicae* Sulzer) alters cellular redox status and is influenced by
631 ascorbate. *Plant, Cell & Environment*, 35, 430-440.
632 Lieutier F., Bermudez-Torres K., Cook J., Harris M.O., Legal L., Sallé A., ... Giron D. (2017). From Plant
633 Exploitation to Mutualism (eds N. Sauvion, D. Thiéry & P. A. Calatayud), pp. 55-109. Elsevier.
634 Louis J. & Shah J. (2013). *Arabidopsis thaliana—Myzus persicae* interaction: shaping the understanding of
635 plant defense against phloem-feeding aphids. *Frontiers in Plant Science*, 4, 213.
636 Malamy J.E. & Benfey P.N. (1997). Organization and cell differentiation in lateral roots of *Arabidopsis*
637 *thaliana*. *Development*, 124, 33-44.
638 Martinson E.O., Hackett J.D., Machado C.A. & Arnold A.E. (2015). Metatranscriptome analysis of fig
639 flowers provides insights into potential mechanisms for mutualism stability and gall induction. *PloS One*,
640 10, e0130745.
641 Morkunas I., Mai V.C. & Gabryś B. (2011). Phytohormonal signaling in plant responses to aphid feeding.
642 *Acta Physiologia Plantarum*, 33, 2057–2073.
643 Mutti N.S., Louis J., Pappan L.K., Pappan K., Begum K., Chen M.S., ... Reeck G.R. (2008). A Protein from the
644 salivary glands of the pea aphid, *Acyrthosiphon pisum*, is essential in feeding on a host plant. *Proceedings*
645 *of the National Academy of Sciences*, 105, 9965-9969.
646 Nicholson S.J., Hartson S.D. & Puterka G.J. (2012). Proteomic analysis of secreted saliva from Russian
647 Wheat Aphid (Diuraphis noxia Kurd.) biotypes that differ in virulence to wheat. *Journal of Proteomics*, 75,

2252–2268.

O'Brien J.A. & Benková E. (2013). Cytokinin cross-talking during biotic and abiotic stress responses. *Frontiers in Plant Science*, 4, 451.

Oksanen J., Blanchet F.G., Kindt R., Legendre P., Minchin P.R., O'hara R.B., … Wagner H. (2013). Package 'vegan'. Community Ecol Package Version 2.

Pan Y., Zhu J., Luo L., Kang L. & Cui F. (2015). High expression of a unique aphid protein in the salivary glands of *Acyrthosiphon pisum*. *Physiological and Molecular Plant Pathology*, 92, 175–180.

Park J.E., Park J.Y., Kim Y.S., Staswick P.E., Jeon J., Yun J., … Park C.M. (2007). GH3-mediated auxin homeostasis links growth regulation with stress adaptation response in *Arabidopsis*. *Journal of Biological Chemistry*, 282, 10036–10046.

Petersen T.N., Brunak S., von Heijne G. & Nielsen H. (2011). SignalP 4.0: discriminating signal peptides from transmembrane regions. *Nature Methods*, 8, 785.

Pierleoni A., Martelli P.L. & Casadio, R. (2008). PredGPI: a GPI-anchor predictor. *BMC Bioinformatics*, 9, 392.

Pointeau S., Ameline A., Laurans F., Sallé A., Rahbé Y., Bankhead-Dronnet S. & Lieutier F. (2012). Exceptional plant penetration and feeding upon cortical parenchyma cells by the woolly poplar aphid. *Journal of Insect Physiology*, 58, 857–866.

Pundir S., Martin M.J. & O'Donovan C. (2017). Uniprot protein knowledgebase. *Protein Bioinformatics: From Protein Modifications and Networks to Proteomics*, 41-55.

R Core Team (2013). R: A language and environment for statistical computing. R Foundation for Statistical Computing, Vienna, Austria. URL http://www.R-project.org/.

Ramsey J.S., Wilson A.C.C., de Vos M., Sun Q., Tamborindeguy C., Winfield A., Malloch G., Smith D.M., Fenton B., Gray S.M., Jander G. (2007). Genomic resources for *Myzus persicae*: EST sequencing, SNP identification, and microarray design. *BMC Genomics*, 8, 423–423.

672 Sallé A., Pointeau S., Bankhead-Dronnet S., Bastien C. & Lieutier, F. (2017). Unraveling the tripartite
673 interactions among the woolly poplar aphid, its host tree, and their environment: a lead to improve the
674 management of a major tree plantation pest? *Annals of Forest Science*, 74, 79.
675 Schaller G.E., Bishopp A., & Kieber J.J. (2015). The yin-yang of hormones: cytokinin and auxin interactions
676 in plant development. *The Plant Cell*, 27, 44-63.
677 Schoonhoven L.M., Van Loon J.J.A. & Dicke M. (2005). Insect–Plant Biology. Oxford University Press.
678 Schulz M.H., Zerbino D.R., Vingron M. & Birney E. (2012). Oases: robust *de novo* RNA-seq assembly
679 across the dynamic range of expression levels. *Bioinformatics*, 28, 1086-1092.
680 Shorthouse J.D., Wool D., & Raman A. (2005). Gall-inducing insects – nature's most sophisticated
681 herbivores. *Basic and Applied Ecology*, 6, 407-411.
682 Stuart J.J., Chen M.S., Shukle R. & Harris M.O. (2012). Gall midges (Hessian flies) as plant pathogens.
683 *Annual Review of Phytopathology*, 50, 339-357.
684 Testerink C. & Munnik T. (2005). Phosphatidic acid: a multifunctional stress signaling lipid in plants.
685 *Trends in Plant Science*, 10, 368-375.
686 Tong Z., Gao Z., Wang F., Zhou J. & Zhang Z. (2009). Selection of reliable reference genes for gene
687 expression studies in peach using real-time PCR. *BMC Molecular Biology*, 10, 71.
688 Tooker J.F. & De Moraes C.M. (2008). Gall insects and indirect plant defenses: A case of active
689 manipulation? *Plant Signaling & Behavior*, 3, 503-504.
690 Tooker J.F. & Helms A.M. (2014). Phytohormone dynamics associated with gall insects, and their
691 potential role in the evolution of the gall-inducing habit. *Journal of Chemical Ecology*, 40, 742–753.
692 Vandermoten S., Harmel N., Mazzucchelli G., De Pauw E., Haubruge E. & Francis F. (2014). Comparative
693 analyses of salivary proteins from three aphid species. *Insect Molecular Biology*, 23, 67-77.
694 Will T., Tjallingii W.F. Thönnessen A. & van Bel A.J. (2007). Molecular sabotage of plant defense by aphid
695 saliva. *Proceedings of the National Academy of Sciences*, 104, 10536-10541.

696 Wu F.H., Shen S.C., Lee L.Y., Lee S.H., Chan M.T. & Lin C.S. (2009). Tape-*Arabidopsis* Sandwich-a simpler
697 *Arabidopsis* protoplast isolation method. *Plant Methods*, 5, 16.
698 Xue H.W., Chen X. & Mei Y. (2009). Function and regulation of phospholipid signalling in plants.
699 *Biochemical Journal*, 421, 145–156.
700 Yang J.L., Yang R., Cheng A.C., Jia R.Y., Wang M.S. & Zhang S.H. (2010). Five-minute purification of PCR
701 products by new-freeze-squeeze method. *Journal of Food, Agriculture & Environment*, 8, 32–33.
702 Yang Y. & Smith S.A. (2013). Optimizing *de novo* assembly of short-read RNA-seq data for phylogenomics.
703 *BMC Genomics*, 14, 328.
704 Zarate S.I., Kempema L.A. & Walling L.L. (2007). Silverleaf whitefly induces salicylic acid defenses and
705 suppresses effectual jasmonic acid defenses. *Plant Physiology*, 143, 866-875.
706 Zerbino D. & Birney E. (2008). Velvet: algorithms for de novo short read assembly using de Bruijn graphs.
707 *Genome Research*, gr-074492.
708 Zhao C., Escalante L.N., Chen H., Benatti T.R., Qu J., Chellapilla S., … & Richards S. (2015). A massive
709 expansion of effector genes underlies gall-formation in the wheat pest *Mayetiola destructor*. *Current*
710 *Biology*, 25, 613-620.
711 Zhao C., Shukle R., Navarro Escalante L., Chen M., Richards S., & Stuart J.J. (2016). Avirulence gene
712 mapping in the Hessian fly (*Mayetiola destructor*) reveals a protein phosphatase 2C effector gene family.
713 *Journal of Insect Physiology*, 84, 22-31.
714

Figure 1: Gene Ontology treemap for the salivary transcriptome of *Phloeomyzus passerinii*. The box size correlates to the number of sequences isolated. Numbers between brackets indicate the number of sequences identified. Green boxes indicate binding proteins, purple boxes indicate enzymes, red boxes indicate structural constituents, the blue box indicates transporters and the brown box molecular transducers. A Detailed list of the proteins can be found in the table S4.

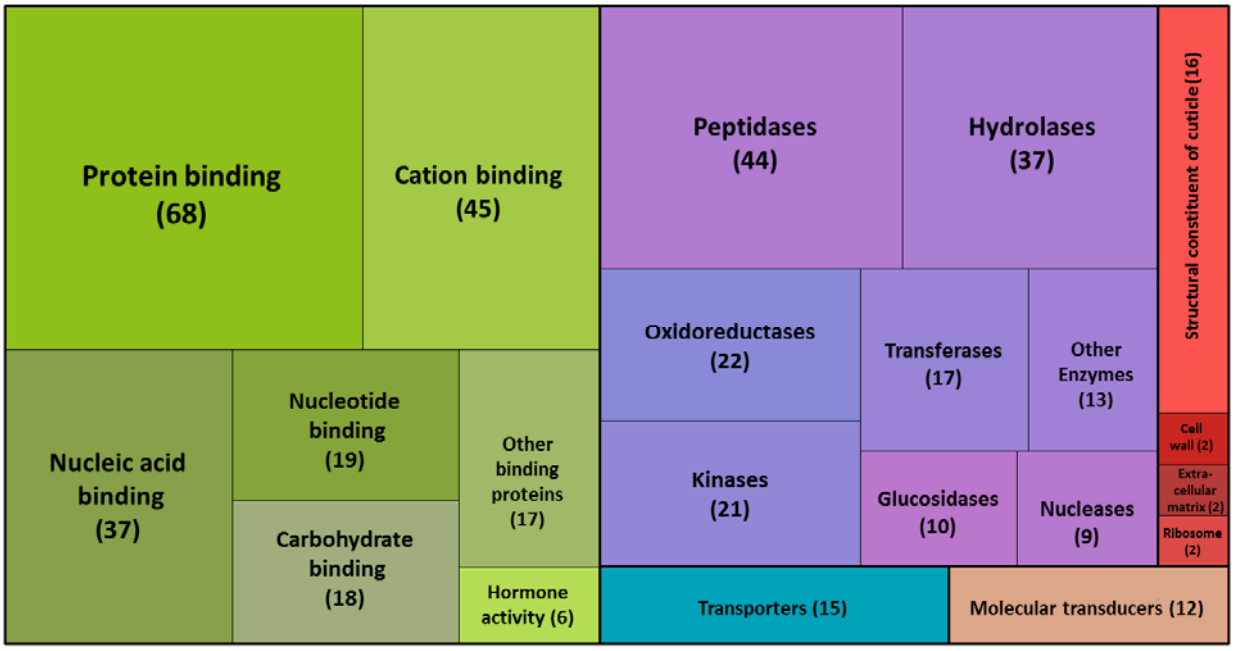

723 **Figure 2:** Representative salivary sheaths secreted in artificial diets by *Phloeomyzus passerinii*. Sheaths
724 stained and observed after 24 h probing in an agarose diet: (A) sheath stained with Coomassie blue; (B)
725 black stained sheaths in diet containing 0.1% DOPA, indicating a phenoloxidase activity, note the dark
726 halo surrounding the upper sheath; (C) reddish stained sheath in diet immersed with 0.1% DAB and 0.1%
727 H_2O_2, indicating a peroxidase activity. Black bars represent 10 µm.
728

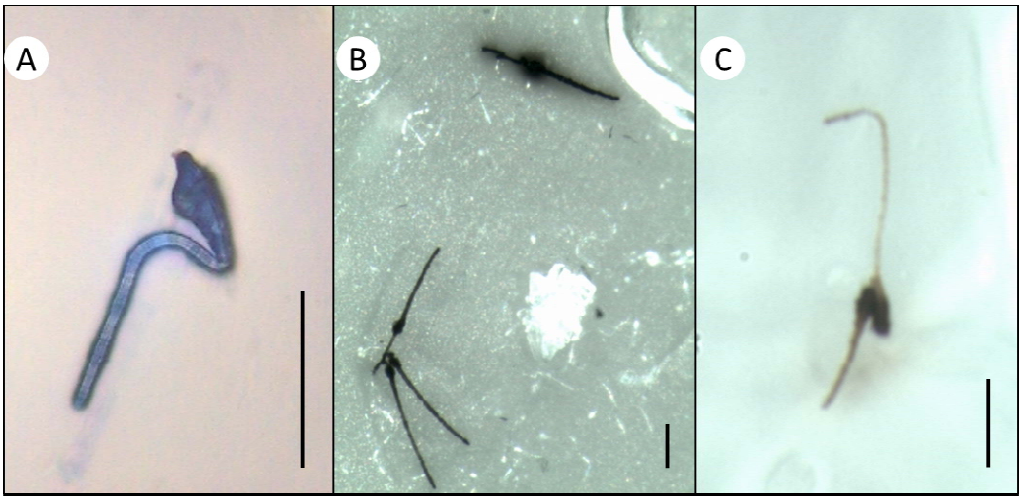

729
730
731

Figure 3: Heatmap of log_2-fold changes of 43 poplar genes belonging to eight different physiological processes or metabolic pathways (lower left box), after incubation of poplar protoplasts of two poplar genotypes (Koster and I-214) with salivary proteins of two aphids (*Myzus persicae* (*M. p.*) and *Phloeomyzus passerinii* (*P. p.*)). Non-host interactions are expected between both poplar genotypes and *M. persicae*, while incompatible interactions are expected between *P. passerinii* and Koster and compatible interactions between *P. passerinii* and I-214. Downregulation appears in blue and upregulation in red. Gene code is presented below the heatmap, modalities (i.e. aphid x poplar genotype combinations are presented on the right of the heatmap). Hierarchical clustering has been built with Euclidean distances.

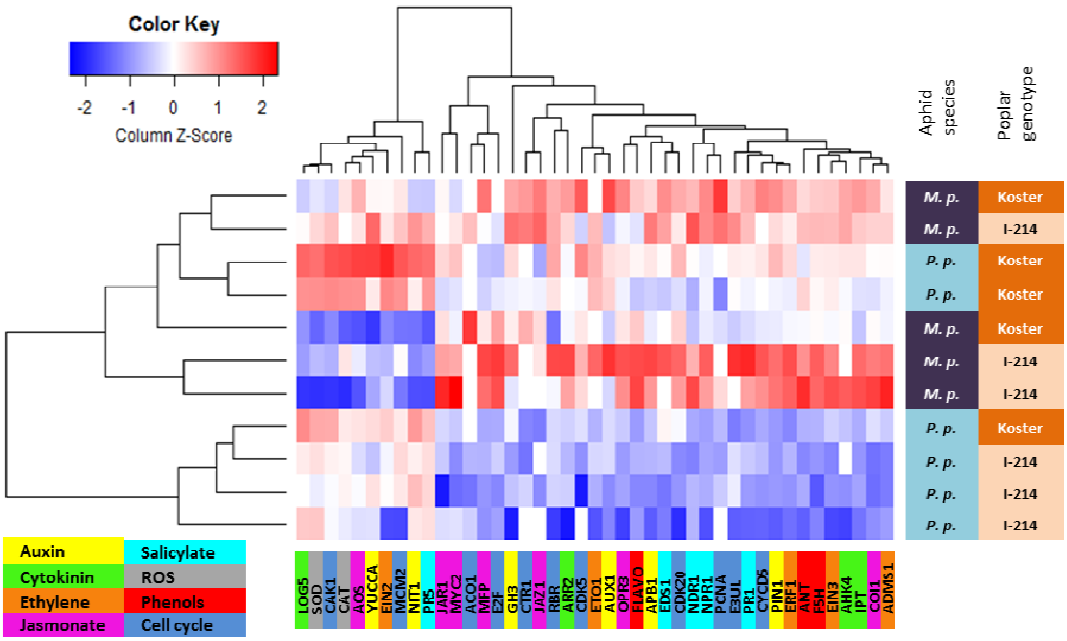

743 **Figure 4:** Fold changes of genes involved in auxin (left) and cytokinin (right) pathways of poplar
744 protoplasts collected from two poplar genotypes (I-214 and Koster), after incubation with salivary
745 proteins of two aphids (*Myzus persicae* and *Phloeomyzus passerinii*). Dots represent the average fold
746 change value, and bars represent credibility intervals.

747

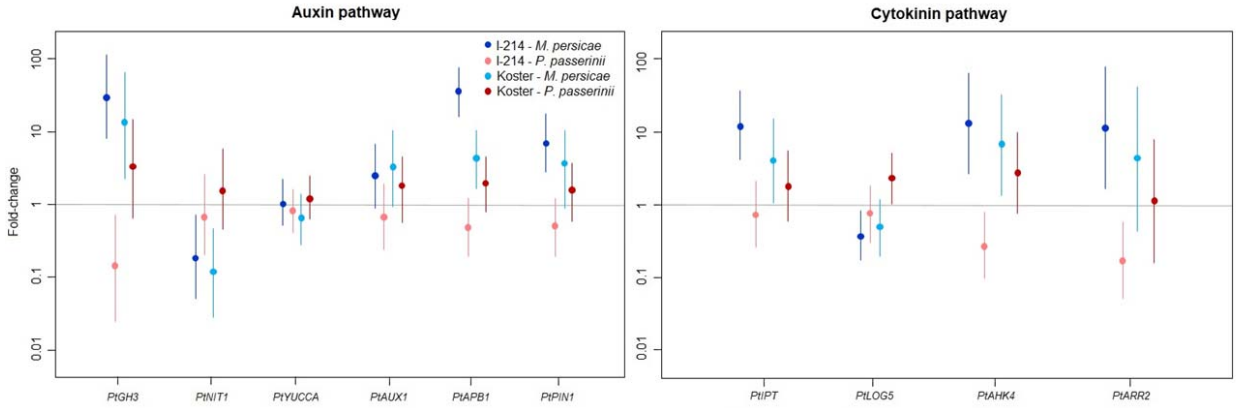

748

749

Figure 5: Representative GUS assays of transgenic seedlings of *Arabidopsis thaliana pIAA2*::GUS, showing whole plants (A, C, E, G, I and K), and root tips (B, D, F, H, J and L), after 3 h of incubation in 20 µM of IAA (A and B), TE/Tween buffer (C and D), and 1 and 10 µg of salivary proteins of *Phloeomyzus passerinii* (E, F, I and J) or *Myzus persicae* (G, H, K and L). Black bars represent 1 mm for whole plants (A, C, E, G, I and K) and 10 µm for root tips (B, D, F, H, J and L). Five seedlings were used for each modality.

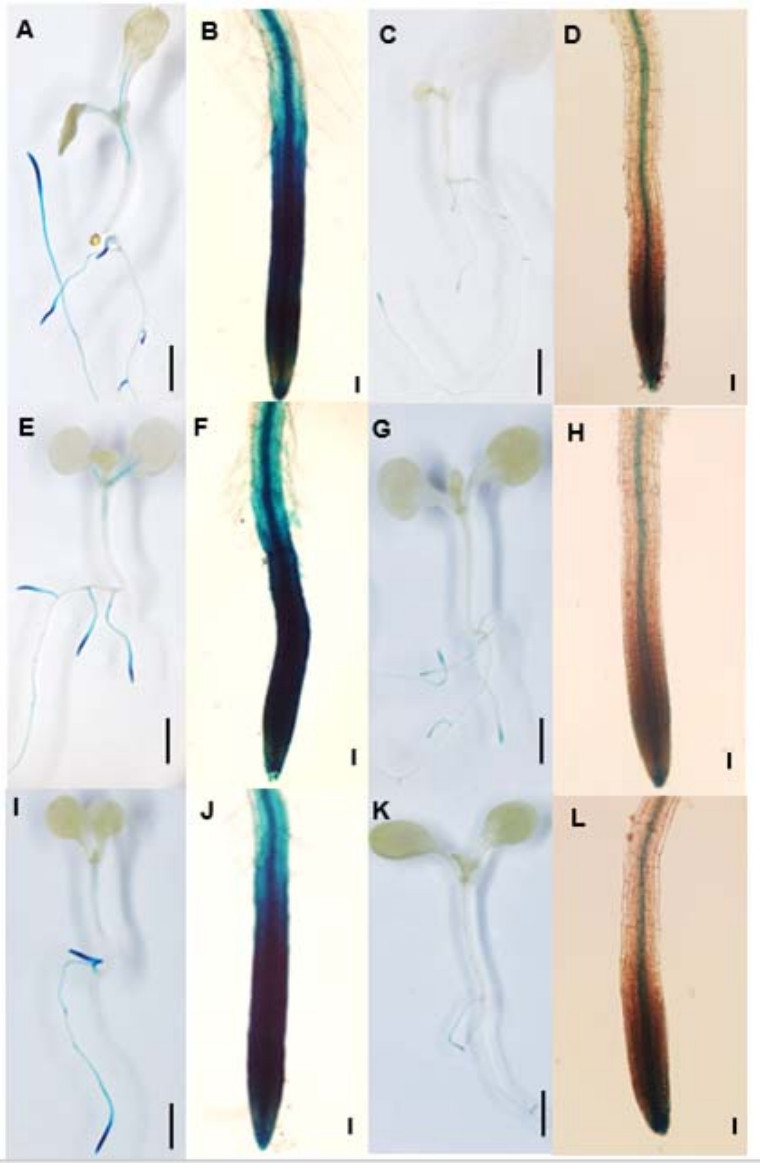

Figure 6: Representative GUS assays of transgenic seedlings of *Arabidopsis thaliana pARR16*::GUS, showing whole plants (A, C, E, G, I and K), and root tips (B, D, F, H, J and L), after 4 h of incubation in 20 µM of BAP (A and B), TE/Tween buffer (C and D), and 1 and 10 µg of salivary proteins of *Phloeomyzus passerinii* (E, F, I and J) or *Myzus persicae* (G, H, K and L). Black bars represent 1 mm for whole plants (A, C, E, G, I and K) and 10 µm for root (B, D, F, H, J and L). Five seedlings were used for each modality.